DESIGN OF A HYDRAULIC SERVO SYSTEM FOR ROBOTIC MANIPULATION

Martin CHOUX and Geir HOVLAND
University of Agder
Department of Engineering Sciences/Mechatronics
4898 Grimstad
NORWAY
Email: martin.choux@uia.no

In this document the design, control and simulation of a hydraulic model for grasping an object is presented. The principal equations that constraint such a system are first investigated through the presentation of the hydraulic components which constitute the model. Their intrinsic characteristics are discussed as well as their interactions with each other. The controller that best fit this application is found to be a hybrid position/force control where the external forces are considered as a disturbance. In the last part of this document the model is simulated with more realistic component parameters including Stribeck effect friction, leakage and nonlinear valve characteristics. The results found with this simplified model show good correlation with the more realistic simulated environment.

Keywords: Hydraulic, Control, Manipulator, Grasping

1 INTRODUCTION

Two important functions of robotic manipulation are to restrain objects and to manipulate objects. Sometimes the functions are called fixturing and dexterous manipulation. One crucial problem in these tasks is the choice of grasp forces F so as to avoid, or minimize the risk of slippage when a turning torque M is applied. However some parameters can change from one object to the other. The friction coefficient or the wear of the gripper are examples of parameters that are difficult to predict. Consequently, the force F needs to be actively adjusted during the grasp and manipulation of the object. Force control is therefore required. Of course the gripper position needs also to be controlled during the first phase of the operation, when the manipulator approaches the object and makes contact. In this document, the manipulation of heavy objects and the transmission of important efforts are considered. One target application is for example the manipulation of drilling pipes on off-shore oil platform. Electrical power is limited due to the fact that ferromagnetic materials saturate at a low flux density, and therefore, the torque output per unit mass of iron in a motor armature is relatively low, whereas fast responses for high-torque devices can be achieved by fluid power. For this reason the objective of this paper is to design, control and simulate a hydraulic servo system for robotic manipulation.

2 SYSTEM COMPONENTS

The schematic of a simple hydraulic system, given in Fig.1, will be used in the following part to describe and analyze the behaviour of the main hydraulic components which form together a common hydraulic system. With the definition of the different parameters and their relationships, the understanding of this simple system constitutes the first step in the design and simulation of the global model.

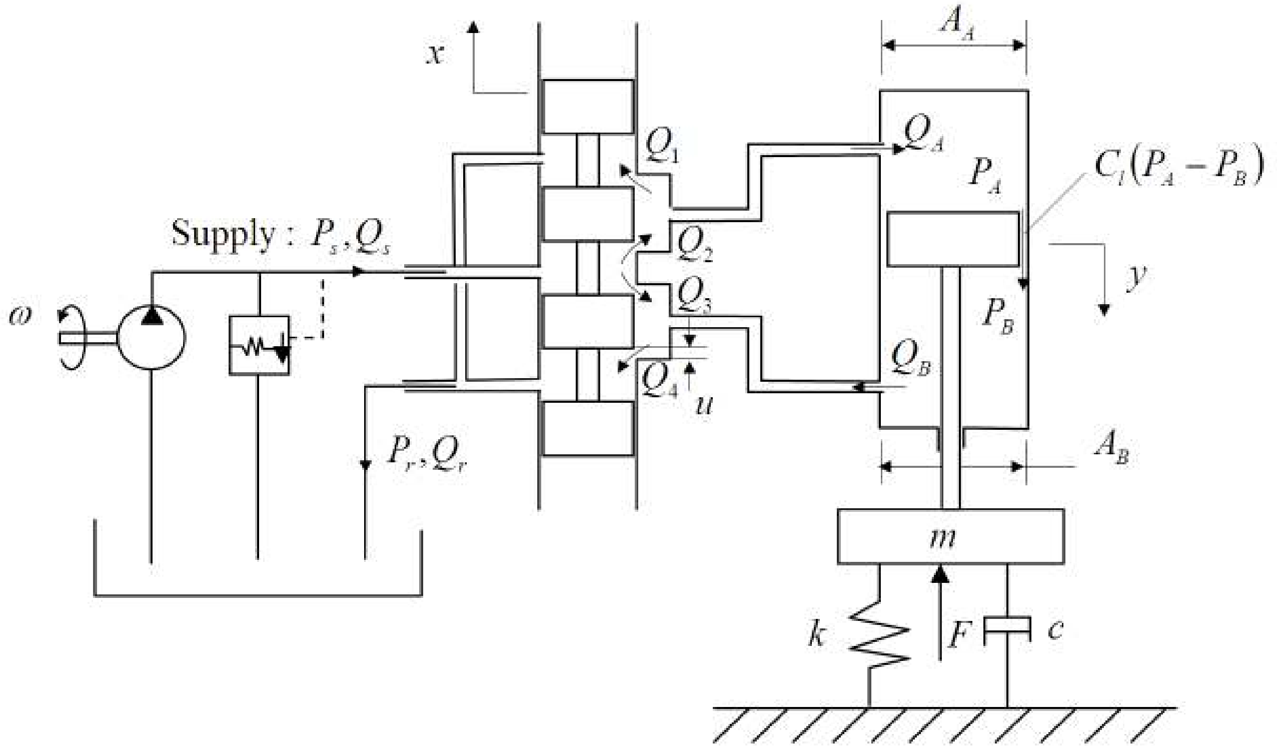

Fig. 1: Schematic of a four-way valve-controlled linear actuator

At the very beginning of the design phase, one must decide how the actuator will be controlled. Either a variable displacement pump or the combination of a constant displacement pump with a proportional control valve can be chosen. In the present grasping application high accuracy and high bandwidth for the servomechanism are preferred to high power efficiency. For this reason a valve controlled hydraulic actuator has been chosen. The system Fig.1 includes a fixed displacement pump (constant volumetric flow rate, volumetric displacement V_p, angular velocity ω), a high-pressure relief valve (desired pressure P_s), a hydro-pneumatic accumulator and a tank in order to supply a pressure P_s and flow Q_s to the rest of the system. A four-way valve (underlapped dimension *u*) distributes the flow to a cylinder where a single rod is connected to the load (mass *m*) and the actuator piston (pressurized area A_A and A_B, leakage coefficient C_l). A load disturbance force F acts against the load. *x* represents the displacement of the spool valve whereas *y* stands for the piston displacement. The two volumetric flow through the actuator are Q_A and Q_B.

2.1 Hydraulic control valve

Valve type There are two types of valve: flow control valve and pressure control valve. Their pressure-flow characteristics are different. For a flow control valve, the objective is to maintain the control flow rate of the valve constant in a certain range of pressure. In the proposed application, the stress is put on the force control, thus a pressure control valve is here chosen.

Change of flow with respect to valve displacement and pressure drop For a turbulent flow through an orifice, the pressure-flow relation can be calculated from the Bernoulli principles

$$Q = AC_d\sqrt{\frac{2}{\rho}P} \tag{1}$$

where A is the discharge flow area of the valve, C_d id the discharge coefficient that must be determined experimentally, ρ id the fluid density and P is the pressure drop across the valve. For zero loss of energy, $C_d = 1$, but in practice the discharge coefficient is in the range $C_d = 0.6 - 0.8$ depending of whether the edges are rounded or not. $C_d = 0.67$ is a good compromise and will be used in the following. The discharge flow area is proportional to the valve displacement.

Symmetric and matched valve, symmetric load In the case where the valve is matched and symmetric and the load is symmetric some simplifications can be made. The symmetric load assumption $Q_A = Q_B$ implies that the load does not accumulate fluid, which means that compressibility effects are not accounted for. This assumption is therefore not consistent with the assumptions that will be used in the derivation of models of hydraulic actuators in the following. However, the assumption of a matched and symmetric valve and a symmetric load leads to a very useful transfer function model for valve controlled hydraulic actuators which represents a good approximation of the system dynamics. It is shown in **Egeland , O.; Gravdahl, T.** (2003) that this assumption implies the equations

$$Q_1 = Q_3, \quad Q_2 = Q_4 \tag{2}$$

and

$$P_s = P_A + P_B \tag{3}$$

if P_r is neglected compared to P_s.
In this case it is convenient to introduce the load pressure

$$P_L = P_A - P_B \tag{4}$$

And the load flow

$$Q_L = \frac{1}{2}(Q_A + Q_B) \tag{5}$$

The load flow can then be expressed by the valve characteristic

$$Q_L = C_d bx\sqrt{\frac{1}{\rho}(p_s - \mathrm{sgn}(x)P_L)} \tag{6}$$

where b = 0.16 mm is the dimension of the valve rectangular orifice.
It is possible to linearize this equation around nominal operating conditions by using the Taylor series.

$$Q = Q_0 + \left.\frac{\partial Q}{\partial x}\right|_0 (x - x_0) + \left.\frac{\partial Q}{\partial P}\right|_0 (P - P_0) \tag{7}$$

where *x* is the generalized displacement of the valve that alters the discharge area, and the subscript 0 identifies the nominal operating conditions of the valve. In order for Eq.(7) to be valid, the actual operating conditions of the valve cannot deviate too far from the nominal operating conditions.

Position Control When controlling the position of an actuator with the valve, a good choice of the operating conditions is to select $x_0 = 0$, $Q_L = 0$ and $P_L = 0$. The linearized flow equation is then given by

$$Q_L = K_{q0} x + K_{c0} P_L \tag{8}$$

where

$$K_{q0} = \left.\frac{\partial Q}{\partial x}\right|_0 = C_d b \sqrt{\frac{2}{\rho} P} \quad \text{and} \quad K_{c0} = \left.\frac{\partial Q}{\partial P}\right|_0 = \left.\frac{b x_0 C_d}{\sqrt{2\rho P}}\right|_0 = 0 \tag{9}$$

For an ideal flow-control valve, the pressure-flow coefficient K_c should be zero, it is however not the case in practice. A more realistic value is obtained by setting the spool in its zero position (*x = 0*) and measuring the leakage flow q_L for a load pressure P_L. The flow-pressure coefficient K_{c0} is then found from $K_{c0} = \frac{q_L}{P_L}$. Simulation with a 5\% underlap valve furnishes $K_c = 0.075\ l/\min/bar$. Using a fluid with a density of $\rho = 900\ kg/m^3$ and a supply pressure $P_s = 100\ bar$, the flow gain at nominal conditions is calculated from Eq.(9): $K_{q0} = 0.82\, m^2/s$.

Force control When the force is controlled instead of the position, the nominal conditions are $x_0 = 0$, $Q_L = 0$ and $P_L = 67\, bar$. The flow-pressure coefficient keep the same value but the flow gain is modified: $K_q = 1.29 K_{q0}$. These values are collected in the following table

Table 1: Linear coefficients

Position control	Force control
$K_c = 0.075 \quad l/\min/bar$	$K_c = 0.075 \quad l/\min/bar$
$K_{q0} = 0.82 \quad m^2/s$	$K_{q0} = 1.05 \quad m^2/s$

These coefficients have a decisive impact in the dynamic performance of hydraulic control systems.

Proportional directional valve It has been shown previously that the load flow Q_L can be determined from the load pressure P_L and the displacement of the valve spool *x*. In order to find the relation between the spool displacement and the electrical signal which operates the system, a closer look into the proportional directional valve has to be taken. First the input signal is amplified with a pulse with modulation (PWM) power control and send to a proportional solenoid with stroke-to-current relationship. The higher the level of the signal coming from the actuation system, the further the control spool is shifted. The valve is equipped with an inductive positional transducer to record the actual position of the control spool. The transfer function between the input signal *u(s)* is typically a second order system:

$$G(s)=\frac{x(s)}{u(s)}=\frac{k_z}{1+2\zeta_v\frac{s}{\omega_v}+\frac{s^2}{\omega_v^2}} \tag{10}$$

where the natural frequency ω_v is 20 Hz and the damping ζ is 0.75. The gain k_z is such that *u*=100 mA gives the maximum spool stroke of 2.5 mm, i.e. $k_z = 2{,}5e-2\, m/A$.

2.2 Hydraulic cylinder

The hydraulic cylinder used in this system has a single-rod piston. It follows that the two area A_A in chamber *A* and A_B in chamber *B,* have different value and the cylinder is not symmetric, $Q_A \neq Q_B$. The volumes of the chambers are given by

$$\begin{aligned} V_A &= V_{A0} + A_A y \\ V_B &= V_{B0} - A_B y \end{aligned} \tag{11}$$

where V_{A0} and V_{B0} are the volumes when the piston position *y* is zero.
The friction forces present in the piston can be described by the Stribeck curve. The result is the sum of three effects, namely the Coulomb friction, the stiction and the viscous friction **Egeland , O.; Gravdahl, T.** (2003). In the proposed model however only the viscous friction will be considered in order to avoid nonlinearities. The viscous friction coefficient *B* is taken equal to 1000 Ns/m. The internal leakage within the cylinder is characterized by the coefficient C_L and the leakage flow is $C_L(P_A - P_B)$.

Load The analysis begins with the load m. The inertia of the actuators is neglected because it is much smaller than the actual forces.

$$m\ddot{y} = (A_A P_A - A_B P_B) - B\dot{y} - F \tag{12}$$

Pressure analysis The compressibility effect of the working fluid is significant for hydraulic actuators. The relation between the differential $d\rho$ in density and the differential dp in pressure is given by

$$\frac{d\rho}{\rho} = \frac{dp}{\beta} \tag{13}$$

Where β is the bulk modulus.
The mass balance for a volume *V* is given by

$$\frac{d}{dt}(\rho V) = \rho q_{in} - \rho q_{out} \tag{14}$$

Insertion of the definition of the bulk modulus (13) leads to the following result:

$$\frac{V}{\beta}\dot{p} + \dot{V} = q_{in} - q_{out} \tag{15}$$

The mass balance for the chambers *A* and *B* of the cylinder in Fig.1 are

$$\dot{V}_A + \frac{V_A}{\beta}\dot{P}_A = -C_l(P_A - P_B) + Q_A$$
$$\dot{V}_B + \frac{V_B}{\beta}\dot{P}_B = -C_l(P_B - P_A) - Q_B \quad (16)$$

Symmetric cylinder with matched and symmetric valve If the load is assumed to be symmetric and the valve is matched and symmetric, $A_A = A_B = A_P$, $V_A = V_B = 1/2V_t$, Eq.(3) gives $\dot{P}_A + \dot{P}_B = \dot{P}_s + \dot{P}_r$ it is then possible to combine the two mass balances into one single mass balance with the load flow Q_L and the load pressure P_L.

$$\frac{V_t}{4\beta}\dot{P}_L = -C_l P_L - A_P\dot{y} + Q_L \quad (17)$$

Eq.(12) becomes

$$m\ddot{y} = A_P P_L - B\dot{y} - F \quad (18)$$

3 CONTROL

In this section the objective is to design a controller that combines position/force control. A review of the basic approaches has been made in 1993 in **Patarinski, S.P.; Botev, R.G.** (1993) where three different ideas are distinguished: hybrid position/force control, impedance control and linear optimal control. The second idea supposes that the environmental stiffness is known and the last idea combines the first two. Since the stiffness of the manipulated object is not known a priori, a hybrid position/force control is selected. Two different controllers are then implemented and a connecting element makes the system switch between them in when required. Example of such hybrid controller can be found in **Clegg, A.C.; Dauchez, P.; Lane, D.M.; Dunningan, M.W.; Cellier, L.** (1997) or more recently in **Sun, P.; Ferreira, J.A.; Grácio, J.J.** (2006) where Fuzzy Logic Control (FLC) is used.

Block diagram Using Eqs.(10), (8), (17) and (18), the block diagram of the system is shown in Fig.2.

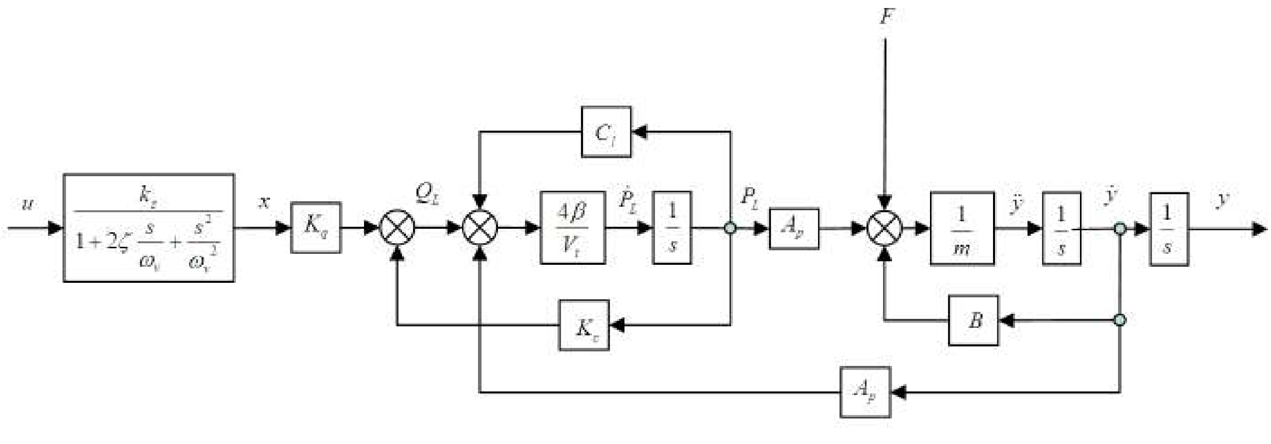

Fig. 2: Block diagram of a valve controlled cylinder

The reduced block diagram in the frequency domain is given in Fig.3

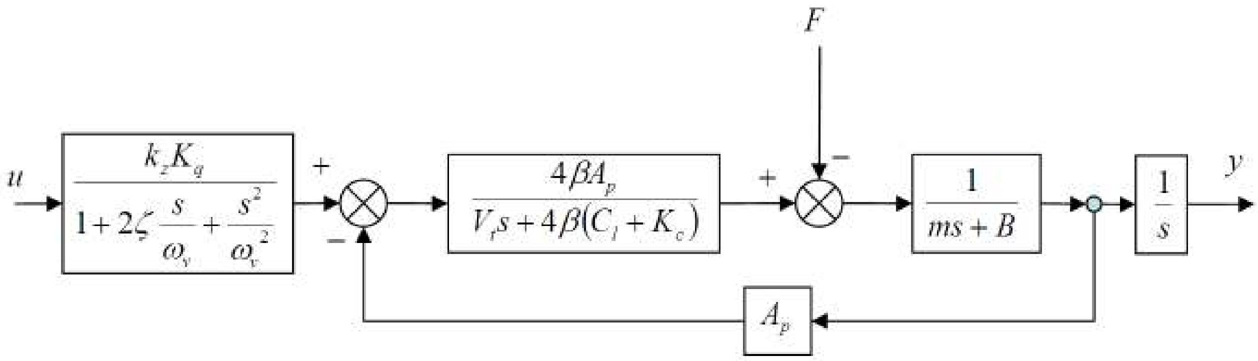

Fig. 3: Reduced block diagram

Controller design In order to find the controller parameters, the transfer functions H_p and H_f are considered:

$$H_p = \frac{y}{u} = \frac{G(s)}{s}\frac{\dfrac{4\beta A_P}{mV_t}}{s^2 + \left(\dfrac{4\beta(C_L + K_c)}{V_t} + \dfrac{B}{m}\right)s + \dfrac{4\beta}{mV_t}\left(B(C_L + K_c) + A_P^{\,2}\right)}$$

$$H_f = \frac{F_m}{u} = G(s)\frac{\dfrac{4\beta A_P}{V_t}\left(\dfrac{B}{m} + s\right)}{s^2 + \left(\dfrac{4\beta(C_L + K_c)}{V_t} + \dfrac{B}{m}\right)s + \dfrac{4\beta}{mV_t}\left(B(C_L + K_c) + A_P^{\,2}\right)} \qquad (19)$$

For the following parameters:

$$\begin{aligned} &m = 10\ kg \quad \beta = 7000\ bar, \quad C_t = 0, \quad K_c = 0.075\ l/\min/bar, \\ &K_q = 0.82\ m^2/s \quad V_t = 0.782\ l, \quad A_P = 14.5\ cm^2, \quad B = 1000\ Ns/m, \\ &k_z = 25\ mm/A, \quad \omega_v = 20\ rad/s, \quad \zeta = 0.75 \end{aligned} \qquad (20)$$

the transfer function H_p is:

$$H_P(s) = \frac{5{,}21e9}{s\left(s^2 + 180s + 1.44e4\right)\left(s^2 + 145s + 7.6e5\right)} \qquad (21)$$

Placing a position sensor on the cylinder, it is possible to make a feedback to the input *u*. The close loop is stable with a 50 deg phase margin and a 10 dB gain margin by adding a proportional corrector $C(s) = 0.55$.

With the same values but $K_p = 1.05 m^2/s$, the transfer function H_f is:

$$H_P(s) = \frac{5{,}21e10(s + 100)}{\left(s^2 + 180s + 1.44e4\right)\left(s^2 + 145s + 7.6e5\right)} \qquad (22)$$

With two pressure sensors on the cylinder, it is possible to make a feedback to the input *u*. The close loop is stable with a 50 deg phase margin and a 12 dB gain margin by adding a proportional integrator corrector $C(s) = \frac{0.0032}{1+5s}$.

Hybrid position/force control Different phases occur successively during the grasping operation. The first is the approach phase, where there is a high velocity/low force relationship as the piston moves with no applied external force only the seal frictional forces are present. The second is the work phase, where the piston has made contact with the object and a low velocity/high force relationship is encountered. The final phase is the return, which is similar to the approach phase. Consequently a hybrid controller needs to be implemented in order to be able to switch between position and/or force control. Fig.4 shows the block diagram of this controller.

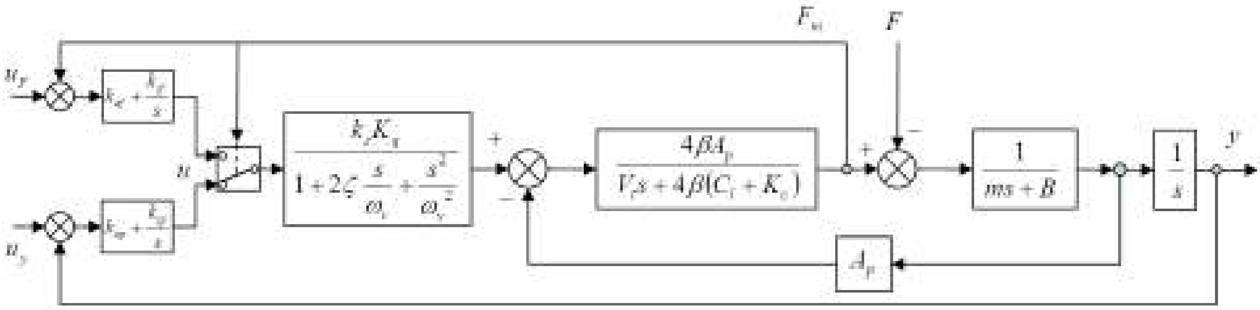

Fig. 4: Hybrid control system

The switcher between position and force control is commanded by the measured force F_m associated with a threshold *T*. When F_m reaches *T*, the controller is switched to force control mode.

4 SIMULATION

In the previous chapter a hybrid control system has been designed based on several assumptions. The load has been supposed symmetric, the valve matched and also symmetric. The classical orifice equation has been linearized around two points with two different operating conditions. In order to verify this model with more realistic environment, in this section the system will be implemented and simulated with the software SimulationX©. The structure is represented in Fig.5. The component EndStop1 is simulating a force disturbance at the load. The pressure in the cylinder chambers are measured and feed back to the force controller as well as the mass displacement to the position controller. The results in Fig.6 show that the system implemented with the controller found previously is stable. The red curve shows the mass position for an input position signal in green. The threshold for which the controller switches from position to force is 8000 N. Note that the position of the load does not reach the desired position because the desired force of 14 kN is reached before.

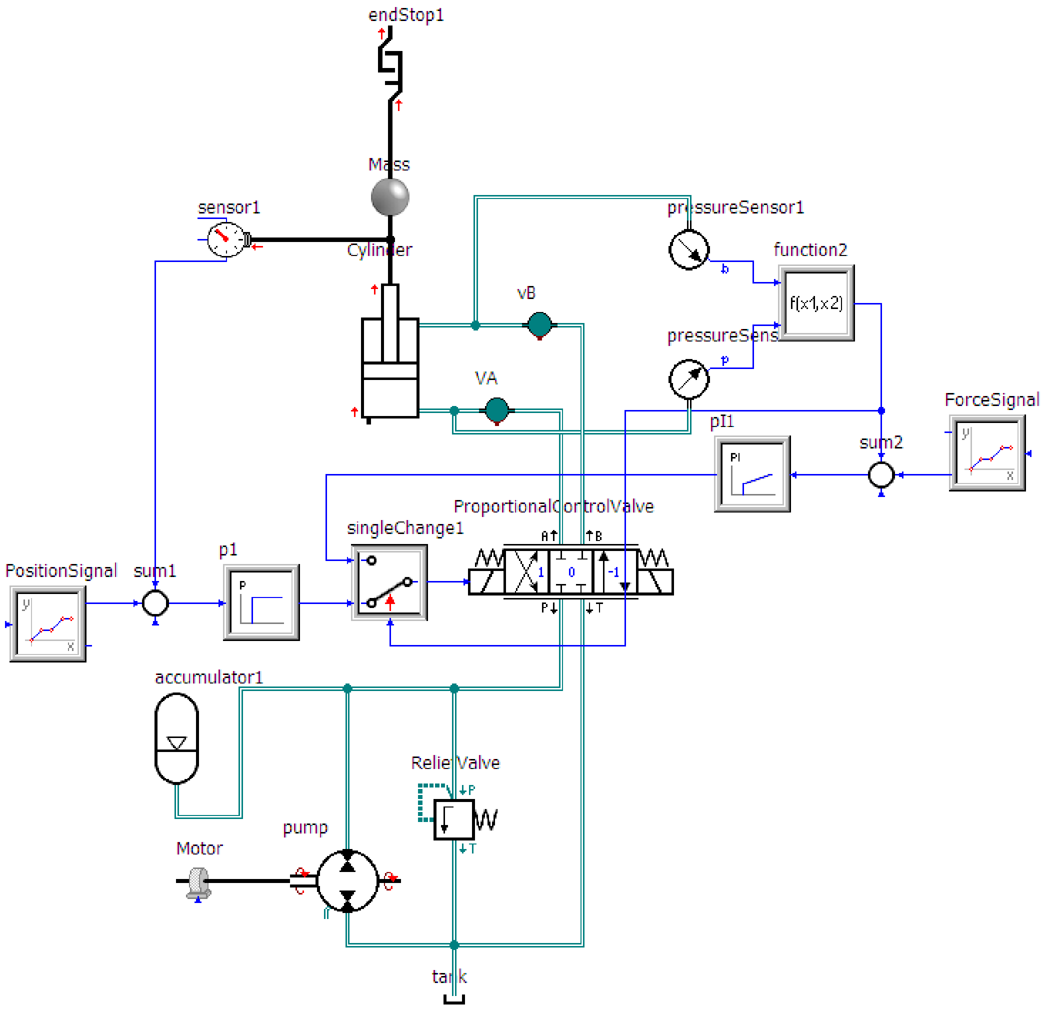

Fig. 5: Hybrid control system

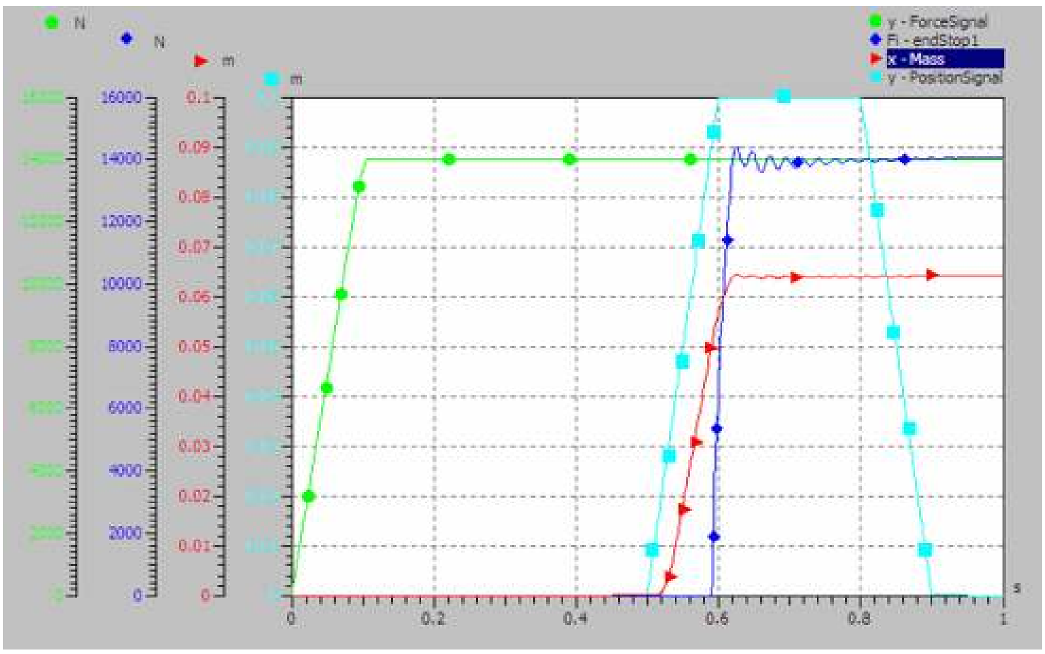

Fig. 6: Position and force of the load

5 CONCLUSION

In this document the design, control and simulation of a hydraulic model for grasping an object is presented. The controller that best fit this application is a hybrid position/force control composed of a proportional corrector for position control and a proportional integrator for force control. The controller switches between these two when the force reaches a fixed threshold. The results of the simulation show a good behaviour of the control system under more realistic environment. Construction of a test bench is planned. Another objective with the robotic hand composed of several fingers is to prevent slippage even if one of the fingers fails (sensor or actuator). A fault-tolerant control system is then needed, where faults can be detected, isolated and estimated and where the controller is automatically reconfigured to be adapted to the faulty situation so that the manipulated object does not slip. Such a system can be designed and implemented with the help of the methods described in **Blanke, M.; Kinnaert, M.: Lunze, J.; Staroswiecki, M.** (2006).

6 REFERENCES

Egeland , O.; Gravdahl, T. (2003). *Modeling and Simulation for Automatic Control.* Marine Cybernetics.

Patarinski, S.P.; Botev, R.G. (1993). Review article. Robot force control: a review. *Mechatronics, Vol. 3, No 4, pp. 337-398.*

Clegg, A.C.; Dauchez, P.; Lane, D.M.; Dunningan, M.W.; Cellier, L. (1997). A comparison between robust and adaptive hybrid position/force control schemes for hydraulic underwater manipulators. *Trans. Inst. MC,Vol. 19, No 2, pp. 107-116*.

Sun, P.; Ferreira, J.A.; Grácio, J.J. (2006). Design and control of a hydraulic press. *Proceeding of the 2006 IEEE Conference on Computer Aided Control Systems Design..*

Blanke, M.; Kinnaert, M.: Lunze, J.; Staroswiecki, M. (2006). *Diagnosis and Fault-Tolerant Control.* Springer.